

Computational design of simulated multi-primary display spectral bands for spectral colour reproduction

Chun-Kai, Chang, Yoko Mizokami and Hirohisa Yaguchi

Graduate School of Advanced Integration Science, Chiba University, Japan

Emails: hibadina0520@yahoo.com.tw; mizokami@faculty.chiba-u.jp; yaguchi@faculty.chiba-u.jp

We proposed an optimal combination of primary spectra in six-primary display to reproduce the great majority of spectra from natural objects. We applied normal distribution function to simulate the basic bands of six-primary display, and then we simulated a large data set by least-squares method created from the product of Standard Object Color Spectra (SOCS) database and the irradiance data of Judd *et al.* [1]. A Good final result was obtained with the averaged root-mean-square error (RMSE) from the simulated sample being 0.0132, demonstrating a significant improvement compared to previous studies. We also compared this method to other multi-spectrum methods (Ajito *et al.* [2], Long and Fairchild [3], and non-negative matrix factorization (NMF)) for an expanded sample of SOCS data. The results showed our proposed method had an appropriately sized area in the CIE (u' , v') chromaticity diagram, also with smooth spectral distribution and good reproduction. The spectral radiance distributions can be reproduced well, especially in natural spectral data with the proposed spectral bands.

Received 22 December 2017; revised 02 April 2018; accepted 17 April 2018

Published online: 27 April 2018

Introduction

In the past 10 years, a vigorous development has seen in display industry, from cathode ray tube (CRT) to liquid crystal display (LCD). The liquid crystal panels evolved from the earlier twisted nematic (TN) [4] to multi-domain vertical alignment (MVA) [5] and in-plane switching (IPS) types. The display devices have become not only thinner, but also with expanded viewing angles [6]. The maximum display resolution has also been advanced, from the previous standard-definition (SD) to high-definition (HD), and then to the current 4K and 8K resolutions, demonstrating significant improvement and evolution. In particular, the advances in wide-gamut displays, namely displays with wider colour gamut have been prominent and rapid.

The development of wide-gamut displays has mainly divided to two directions. One is changing the display module to enhance the display colour gamut. For example, from the most traditional cold cathode fluorescent lamp (CCFL) used by liquid-crystal display (LCD) to the current active-matrix organic light-emitting diode (AMOLED) displays, the displayable gamut has increased by a factor of roughly 1.3 relative to the sRGB colour space [7]. The other is expanding the range of displayed colours through adding primary colours to the panels. It is also called the multi-primary display technology. For example, König *et al.* proposed a method for defining the physical dimension of multi-primary display [8]. Over the past decade, increasingly intense research efforts and industrial investment have been devoted to this area [9-16]. As a result, four- and five-primary colour displays are now available in marketing.

With the development of multi-primary display technology, correct colour reproduction for display devices has become a key topic. In particular, effective spectral colour reproduction has become increasingly important as the display panels, colour filters, and backlights continually evolve. Because of the wider colour gamut, this technology is widely used in many areas nowadays. These examples include the reproduction of object surface textures, materials, ancient relics, and paintings; or applications in new light sources, such as light-emitting diodes (LEDs) and organic LEDs (OLEDs) backlights, which could reproduce more colours rather than traditional backlights.

Multi-primary displays also have great potential for more accurate colour reproduction. They can precisely represent the spectral property of objects and scenes with their multiple channels. Sometimes the colour appearance of the devices does not match even when the measured colorimetric values, such as CIE (x , y) or CIELAB are the same. This is due to metamerism in the power distributions associated with observers with different spectral sensitivities. Although multi-primary displays can never completely solve the problem of metamerism, it can produce a spectrum at each pixel in order to be closer to that of the original scene. For this purpose, spectral reproduction is important as it can achieve the best colour reproduction and largely reduce the problem of metamerism. In this article, we focus on the combination of primary colour spectra that can most adequately reproduce the spectra of natural objects in a multi-colour environment.

Generally, the object colours perceived by the human eye could not be perfectly reproduced by displays due to colour gamut limitation. In a previous work, we developed an algorithm of RGBCMY six-primary display, and our computational simulations revealed the reproduction phenomenon of the object colours changing their saturation [17]. Among the six kinds of colour reproduction methods with different objectives as defined by Hunt [18-19], the spectral and preferred colour reproductions are the most difficult approaches for achieving a perfect reproduction. Therefore, in this study, we concentrate on the spectral reproduction in displays and determine the optimal combination of six primary colour spectra by using mathematical methods.

Similar approaches have been used by other researchers. Ajito *et al.* and Long and Fairchild used two projectors with different colour spectrum combinations to reproduce six primary colours and discussed the reproducibility of object colours or existing colour chips [2-3]. Ben-Chorin *et al.* used the singular value decomposition (SVD) method based on colour chips to find the foundations of natural colours, and then used the non-negative matrix factorization (NMF) method to obtain multi-primary combinations [20]. Their results were shown to have the smallest differences from natural colours among five to seven combinations. More recently, this approach has been used to design a real multi-primary display [21], and the colour differences between the reproduction and the sampled pictures were extremely small.

The above explanations concern the reproduction of multispectral and multi-colour data. Compared to theories mentioned above, the approach proposed in this study presents two radical

features. Firstly, different from some previous studies that used the entity colour filters as the basis spectra to reproduce the spectral radiance distribution of object [10, 21-22], our multispectral design concept of this study is based on the primary colours of a simulated six-primary display we had developed [17]. Therefore, in designing the initial values of the spectra, we used mathematical methods to establish six spectra, for which six primary colours (Red, Green, Blue, Cyan, Magenta, and Yellow) at their corresponding positions in the visible light spectrum were considered. Secondly, the reference samples used in this study are obtained via combining natural reflectivity data and light sources. The reflectivity data came from the Standard Object Color Spectra (SOCS) database published by the Japanese Industrial Standards Association in 1998 [23], which contains a total of 54240 colours obtained from the nature world. Some of the previous studies used fewer than 500 sets of reference data, possibly affecting the accuracy of the final results. In contrast, we used more than 3000 reflectance samples taken from the SOCS data. Daylight data from the work of Judd *et al.* [1] was used for the light sources. However, since we used the Matlab software package in this study, calculation with all combinations of light sources and reflectance data would be quite time-consuming without using a supercomputer. Therefore, the colour temperature of the daylight illumination was sampled in the 4000–9000 K range at intervals of 1000 K, in order to ensure that the spectral results can completely reproduce most of the natural colours.

The NMF method is a common solution for modelling multispectral data. Giving the spectral data that must be completely reproduced, this method can be used iteratively to obtain the best combination set. Nevertheless, the obtained result is only for the given sample data, which probably could not completely reproduce the primary colours of light sources in the real world. Hence, we started from the perspective of a variable-wavelength light source, using a normal distribution function (similar to a bell-shaped distribution) to simulate each colour spectrum and fixed the hues of the RGBCMY colours. The normal distribution was determined by adjusting the σ (width) and μ (wavelength) variables. In consider of all possible spectral combinations, no iterative method was used in the calculations.

Construction of target spectra

Colour reflectance data

Firstly, we provided a detailed description of the data used in this study. In Introduction, it was noted that some studies expanded display colour gamut and the achievement of higher display resolution allowed some devices to reproduce the colours of natural objects. However, these reproductions were imperfect due to a small number of sampling. Therefore, we chose the SOCS database as our golden sample. The SOCS database is a spectral reflectance database containing 54240 spectra of objects including Faces, Flowers, Graphics, Krinov Data, Leaves, Paints, Pigments, Photos, Printers, and Textiles. The size of each SOCS category is listed in the second column of Table 1. We chose a total of 3725 colours from all categories, which excluded the Krinov dataset due to its incomplete wavelength sampling. We extracted almost all of the categories with fewer samples as Flowers, Leaves, Paints, and Pigments (the third column of Table 1). For the Faces category, different skin colours were extracted (races: African, Caucasian, and Asian) including both genders and different parts of the face. We only extracted representative samples for the Graphics, Printers and Textiles categories. Figure 1 shows the plots of all selected spectral reflectance data under D65 daylight on the CIE (u' , v') chromaticity diagram, indicating that the distribution exceeds the sRGB colour gamut.

Next, we used the data within the wavelength range of 400–700 nm for principal component analysis (PCA). Because the general spectral reflectance was measured by measuring instruments, in addition to big errors on the low- and high-frequency ends, the spectral reflectance itself also had some non-smooth parts. This would result in additional errors, so we used the first 3 principal components of SOCS as whole spectral radiances instead of the original SOCS data. The method of PCA was proposed in 1901 by Karl Pearson and was developed by Harold Hotelling in 1933 [24]. Its main purpose is to find a linear combination of variability, that the PCA values possess their original variable information. The most important thing is, it could replace the original variable information by few of non-overlapped PCA values.

Categories	Number of assembled data	Number of chosen data
Faces	9461	280
Flowers	148	148
Graphics	30624	438
Krinov Data	370	0
Leaves	92	92
Paints	336	336
Pigments	231	229
Photos	2304	632
Printers	7856	855
Textiles	2818	715
Total	54240	3725

Table 1: Number of data for each category in SOCS database.

We found that the first three principal components and the mean of selected SOCS data, shown in Figure 2, could represent all reflectance data well with the respective contributions of 54%, 22%, and 14%. For more accurate reproduction of spectral reflectance, additional principal components accounted for most of the remaining 10% variability in the data. The 4th, 5th, and 6th components accounted for additional 4%, 2%, and 1.4% of the variance, respectively. While the 4th principal component is not negligible, previous studies have employed three components for analysis [25-27].

Furthermore, it has been suggested that three components are necessary and sufficient [28-29]. Moreover, the inclusion of more principal components would incur high-order and very complex calculations, which may introduce errors and preclude us from finding the best combination of bands. Therefore, only the first three principal components were used in this study.

The reproduction of reflectance data (RE) can be described as in Equation 1. R_1 , R_2 , and R_3 indicate its first three principal components, and \bar{R} denotes the mean of all the data we used. N_1 - N_3 are the weight values obtained from target reflectance, using the least-squares method. The next step is assessing the closeness between the original (OR) and reproduction (RE) data by using the root-mean-square error (RMSE) as shown in Equation 2.

$$RE = (N_1 R_1 + N_2 R_2 + N_3 R_3 + \bar{R}) \quad (1)$$

$$RMSE = \sqrt{\frac{(OR_1 - RE_1)^2 + (OR_2 - RE_2)^2 + \dots + (OR_n - RE_n)^2}{n}} \quad (2)$$

where n has a value of 31 to correspond to the 31 wavelengths between 400 and 700 nm in 10-nm intervals that were sampled in a spectrum.

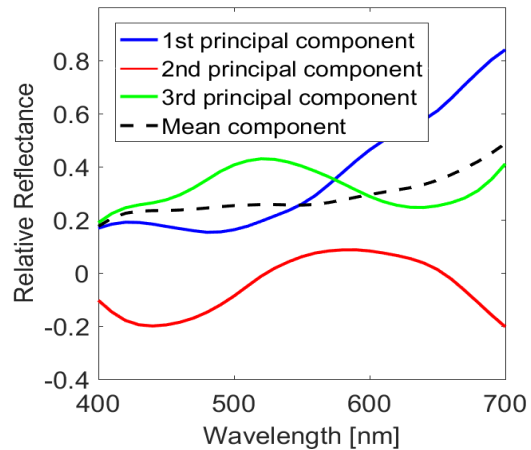
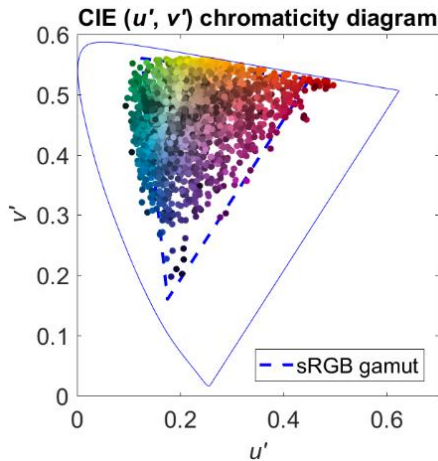


Figure 1 (left): Colour distribution of selected SOCS data.

Figure 2 (right): The first three principal components and the mean of selected SOCS data.

Then, we compared our PCA data (shown in Figure 2) to that reported by Vrhel *et al.* [30], whose dataset contained 354 artificial and natural objects. We used the method of quartiles to examine the averaged RMSE distribution for both dataset. The comparison is shown in Table 2. For clear presentation, the averaged RMSE values are multiplied by a factor of 100. The median averaged RMSE values for our data and Vrhel *et al.*'s data are 1.4169 and 1.2401, respectively. The overall averaged RMSE values are less than 3.2 in both cases.

PCA Method	First quartile (Q ₁)	Median (Q ₂)	Third quartile (Q ₃)
Proposed	0.6375	1.4169	2.3867
Vrhel <i>et al.</i>	0.4044	1.2401	3.1925

Units: averaged RMSE × 100

Table 2: Comparison of results from the proposed method and Vrhel *et al.*'s method.

Illumination data

Secondly, Equations 3-6, derived by Judd *et al.* [1] in 1964 were used to obtain the spectral distribution of daylight data. The colour temperatures were divided into two parts: a lower region of 4000-7000 K and a higher region of 7000-25000 K. These data can also be represented by the PCA results (S_D). The distributions of S_0 , S_1 , and S_2 (the average of the daylight data, the first principal component, and the second principal component, respectively) are shown in Figure 3. Here, T_c denotes the colour temperature, x_D and y_D represent the CIE (x, y) colour coordinates, M_1 and M_2 are the weight values of S_1 and S_2 , respectively.

Region of 4000-7000 K:

$$x_D = -4.6070 \frac{10^9}{T_c^3} + 2.9678 \frac{10^6}{T_c^2} + 0.09911 \frac{10^3}{T_c} + 0.244063; y_D = -3.000x_D^2 + 2.807x_D - 0.275 \quad (3)$$

Region of 7000-25000 K:

$$x_D = -2.0064 \frac{10^9}{T_c^3} + 1.9018 \frac{10^6}{T_c^2} + 0.2478 \frac{10^3}{T_c} + 0.237040; y_D = -3.000x_D^2 + 2.870x_D - 0.275 \quad (4)$$

$$M_1 = \frac{-1.3515 - 1.7703x_D + 5.9114y_D}{0.0241 + 0.2562x_D - 0.7341y_D}; M_2 = \frac{0.0300 - 31.4424x_D + 30.017y_D}{0.0241 + 0.2562x_D - 0.7341y_D} \quad (5)$$

$$S_D = S_0 + M_1S_1(\lambda) + M_2S_2(\lambda) \quad (6)$$

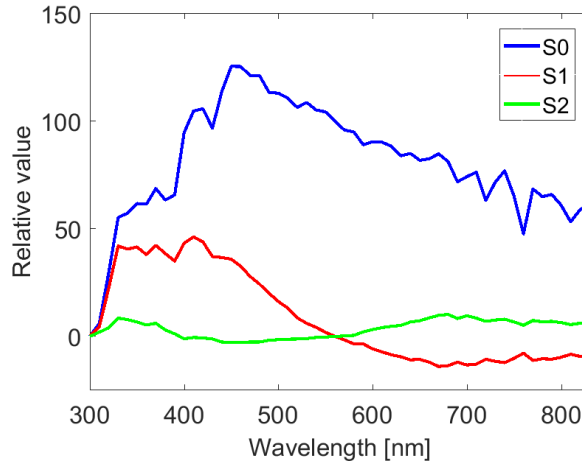


Figure 3: Colour distribution of selected SOCS data.

Multiplication of reflectance and illumination data

Thirdly, we used Equation 7 to obtain the target spectra (O), the spectral radiance distribution, which was acquired via multiplication of the SOCS data and daylight data defined above, in order to form spectral radiances. The reproduction of reflectance data is defined in the same way as in Equation 1. Although the colour temperature range specified by the Equations 3 and 4 is 4000-25000 K, we chose the range of 4000–9,000 K sampled at 1000 K intervals as our source for preparing the radiance data. The wavelength range was from 400 to 700 nm at 10-nm intervals. Although it would be ideal to choose a small wavelength interval of 1-nm intervals, considering the calculation time and minor errors that may ensue, we performed our calculation using 10-nm intervals.

$$O = (N_1R_1 + N_2R_2 + N_3R_3 + \bar{R}) \times (S_0 + M_1S_1 + M_2S_2) \quad (7)$$

Design of six-primary spectra using the target spectra

The combination of multi-spectrum colour filter

To precisely reproduce the target spectra, we used software to simulate the spectral transmission characteristics of the colour filters. Depending on the computational cost, Gaussian functions are usually used to simulate the spectral transmission spectra in given illumination. In this case, we used the normal distribution function ($F_i(\lambda)$), which is a more restricted case of Gaussian function as shown in Equation 8. λ refers to the random probability density in the wavelength range 400-700 nm, and $i = 1 - 6$ labels the six bell curves. μ indicates the dominant wavelength position, and σ specifies the half width at half maximum (HWHM) of the spectrum.

$$F_i(\lambda) = \frac{1}{\sigma_i\sqrt{2\pi}} \exp\left(-\frac{(\lambda-\mu_i)^2}{2\sigma_i^2}\right) \quad (8)$$

Therefore, to stress the spectral radiance distribution, assuming the light spectral distribution of display backlight is a flat distribution of D65, the relationship can be expressed as Equation 9. Because of the light source has a nearly uniform spectral distribution, each spectral radiance distribution of $P_i(\lambda)$ will be an approximately smooth bell curve.

$$P_i(\lambda) = F_i(\lambda) \times (\text{D65 flat light spectral distribution}) \quad (9)$$

For example, we simulate two filters with different spectral transmittance characteristics but at the same wavelength, denoted as F_{i1} and F_{i2} in Figure 4. Assuming the display backlight is D65, the wavelengths (μ) of these two spectral transmittances are set to the same value of 520 nm, and the values of σ_{i1} and σ_{i2} are set to 20 and 50, respectively. For the P_{i1} filter, $(L1^*, a1^*, b1^*) = (62.28, -135.89, 51.48)$ and the chroma is 145.32; for the P_{i2} filter, $(L2^*, a2^*, b2^*) = (83.76, -71.03, 20.26)$ and the chroma is 73.86. When two spectral transmittances are at the same wavelength, a smaller half-width corresponds to a more vivid colour perception.

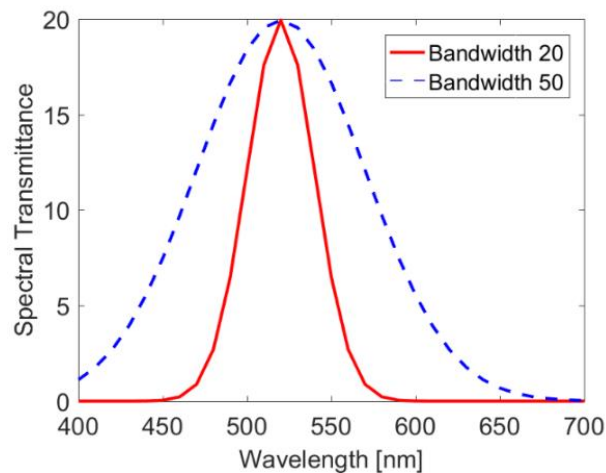


Figure 4: Band distributions of F_{i1} and F_{i2} .

The values of n_1 – n_6 in Equation 10 were obtained using the least-squares method applied to the spectral radiance distribution of the target sample (SRD). Each P_i term in Equation 10 ($i = 1$ – 6) is a spectral radiance distribution as defined in Equation 9. The n_1 – n_6 terms are the spectral intensity of each distribution corresponding to the target spectrum. This adjustment was based on normalised spectral data, although the actual digital counts to reproduce target spectrum was determined by the calibration of the device.

$$SRD = n_1P_1 + n_2P_2 + n_3P_3 + n_4P_4 + n_5P_5 + n_6P_6 \quad (10)$$

Estimation

In this study, we want to create a set of spectral radiance distributions that can be easily simulated by a mechanical or mathematical model, the six-primary spectra are also composed of smooth spectra. The relationship between six-primary spectra and target sample can be expressed as Equation 11. In the ideal case, the parameter O in Equation 7 is approximately equal to SRD in Equation 10.

$$SRD \cong 0 \quad (11)$$

To comply with the colour reproduction method of a realistic display, we used the least-squares method to reproduce the target spectral radiances, by minimising the difference between the reproduced and real data.

In the following, we will describe how this technique was used to simulate the spectral distribution in the nature world. To achieve the best reproduction of all spectra in nature world, we performed several statistical and mathematical methods to find the combination of basic spectra that is optimal for reproducing the entire range of spectra in nature.

The designed six-primary spectra

As mentioned in previous paragraphs, we employed an algorithm that took the normal distribution function to simulate six smooth bell-curve spectra, using the loop instruction of Matlab software to estimate the reproduction. Due to the large amount of the loop data, we separated the analysis to 3 steps. We calculated the averaged RMSE and the *CIEDE2000* ΔE_{00} [31] values between the original and reproduction data in all selected samples (the SOCS data of 3725 spectral reflectance samples multiplied by six irradiance data sampled in the 4000-9000 nm range in 1000 nm intervals). Thus, a total of 22350 data points was considered. The *CIEDE2000* criterion does not take the observer metamerism into account. That is because our sole aim here is to determine whether the radiance distributions of the spectra are completely reproduced.

We started by fixing each band at a wavelength μ ranging from 400 to 700 nm with intervals of 50 nm, and the width of the spectrum σ is set at 30 nm.

In the first step, we varied the wavelength of each band by increasing it by 0-50 nm in intervals of 10 nm and obtain the minimum averaged RMSE. Due to the small impact from the 400- and 700-nm bands on the reproduction, we decided to fix these two bands temporarily to reduce the computational cost.

The second step is the micro-adjustment step. To find more accurate positions for each band obtained from the first step, we varied both μ and σ in the range of ± 10 nm. In this step, the bands at 400 and 700 nm are fixed as well.

Having obtained highly precise positions for the bands, in the final step we only adjusted the magenta bands. The magenta bands are composed of two bands, whose initial positions are at the extremely short wavelength of around 400 nm and the longest wavelength of around 700 nm. As the shapes of the magenta bands could easily affect the reproduction results, we were required to adjust not only μ and σ , but also their height ratio H at the same time. In the moment, we varied both the μ and σ values in the range of ± 50 nm for each band, and the H ratio within the range of 0 to 1000 in intervals of 50.

Results

From Figures 5(a)-5(c), the averaged RMSE values after the first, second, and third steps are 0.0164, 0.0143, and 0.0132, respectively. Therefore, each step further improves the reproduction. The final average of *CIEDE2000* is 0.08. From both the RMSE and *CIEDE2000* results, the reproductions

are very close. The CIE (u' , v') chromaticity diagram is presented in Figure 5(d), showing that the area surrounded by the primary colour of six bands is significantly larger than the SOCS boundary except for the boundary at green region, demonstrating a high capacity to reproduce the colour of natural objects. We tried to make the spectra of green or cyan colours narrower to expand the boundary of the primary colour of six bands, but the result of averaged RMSE values against the sampled SOCS data increased. Thus, we did not further pursue this spectra combination.

Figure 6 compares the averaged RMSE values obtained in three steps (for a clear presentation, the RMSE values have been multiplied by 100). The error bars indicate the 95% confidence interval of the entire dataset. Also noted that with smaller error bars, the data are more concentrated, being closer to the 95% confidence interval.

We also presented the best and worst fits with their individual primary spectrum distributions in Figure 7, with the averaged RMSE values of 0.004368 and 0.04291, respectively. The final (μ , σ) best values for the six bands are (410, 16), (447, 24), (491, 28), (550, 30), (622, 34), (692, 32), and (716, 8); and the H ratio of the magenta bands is 11:15.

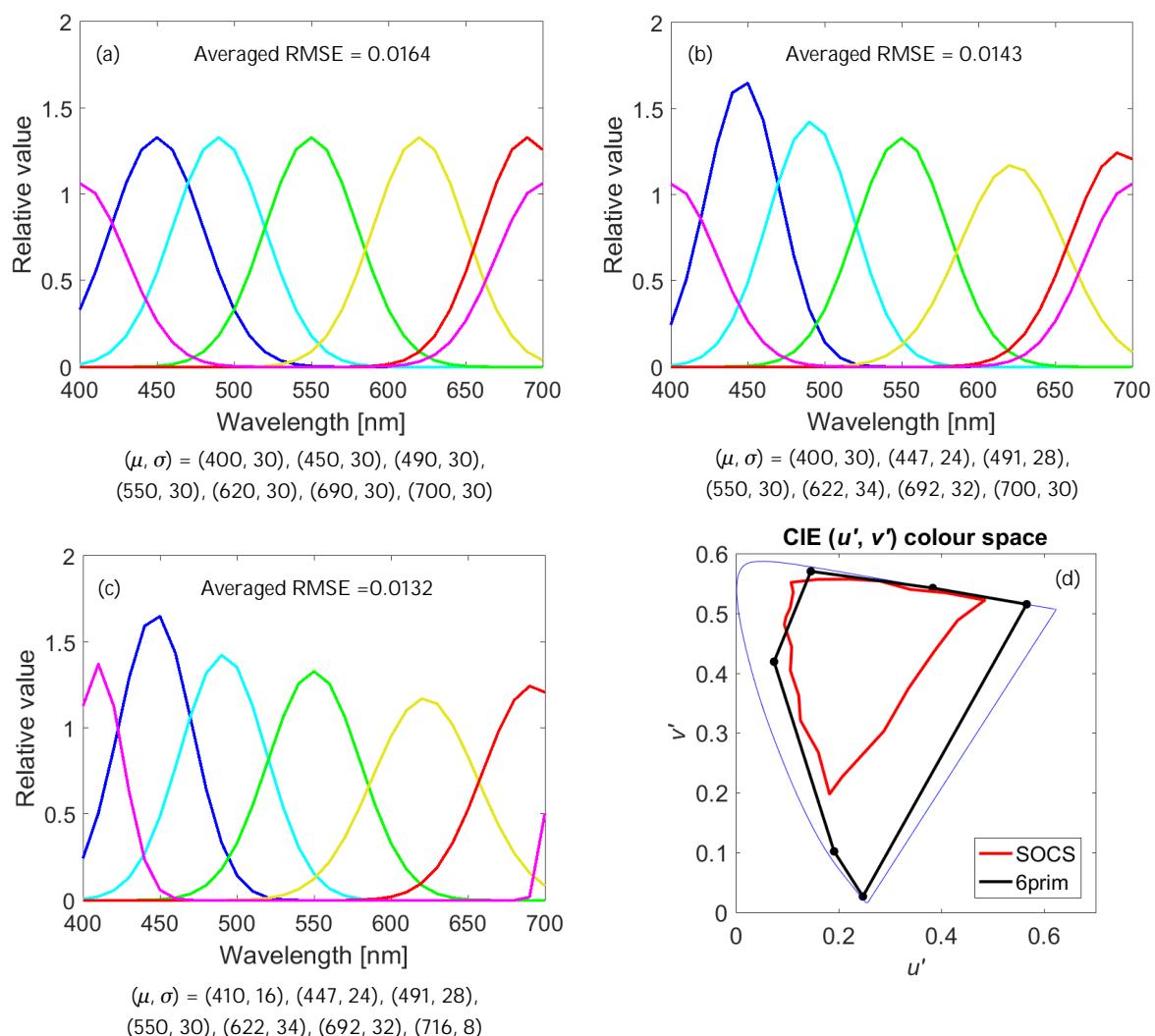


Figure 5: Results of the (a) first, (b) second and (c) third steps; and (d) six-primary and SOCS boundaries on CIE (u' , v') chromaticity diagram.

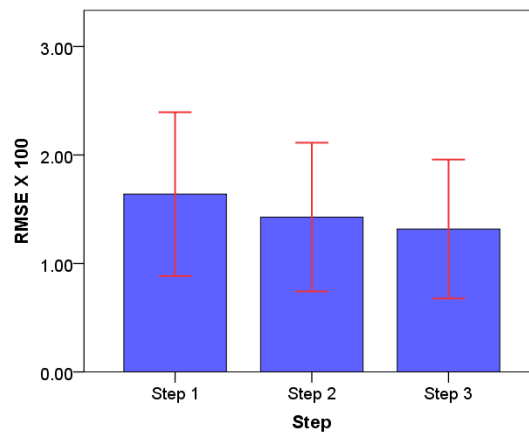


Figure 6: Comparison of averaged RMSE values for the first, second and third steps.

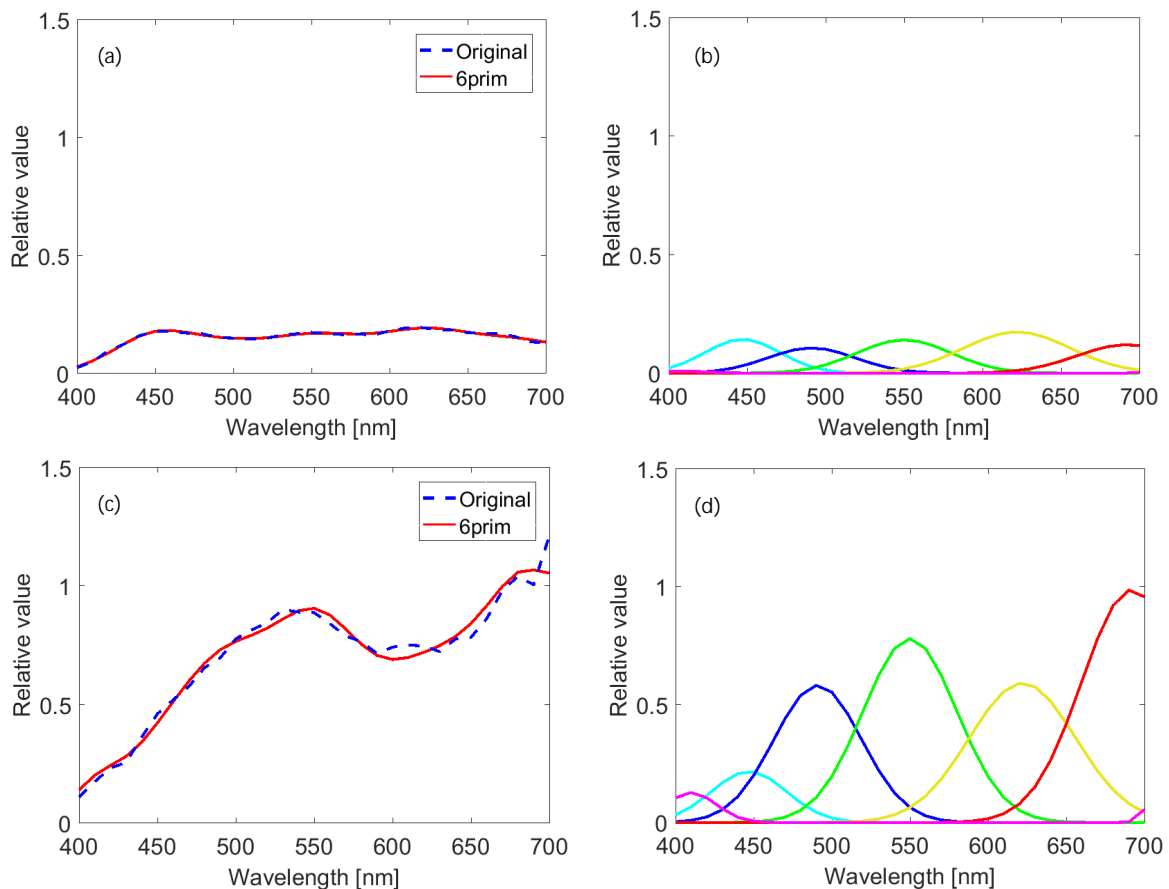


Figure 7: (a) Best fit of the original spectra with six primary spectra; (b) best fit distributions of the six-primary spectra; (c) worst fit with the original and six-primary spectra and (d) worst fit distributions of the six-primary spectra.

Discussion

We now compare our method with other reported six-primary band methods. Ajito *et al.* [2] used two real projectors to construct the six-primary spectra in order to obtain a wide colour gamut. Therefore, their purpose is different from our current study which is obtaining the best reproduction of natural spectra. Nevertheless, this method is used for comparison to ours, because (1) there are very few published studies on six-primary colour spectra and (2) the paper is frequently cited in Long and Fairchild [3]. As Ajito *et al.* [2] did not report any spectral distribution data, we used transparent grid

paper to establish the coordinates, and took data at 10-nm intervals within the wavelength range of 400-700 nm to reconstruct the band distribution shown in Figure 8a. The study by Long and Fairchild [3] had a similar aim to the present study, and undoubtedly produced better averaged RMSE results than ours. The spectra were constructed using the Gaussian distribution, but with no merged bands for the magenta colour shown in Figure 8b. In order to check the reproductivities of the three methods from Ajito *et al.* [2], Long and Fairchild [3], and our proposed method, we compared these reproduction results obtained for the SOCS samples and the Macbeth ColorChecker. The display backlight was assumed as a D65 flat light spectral distribution.

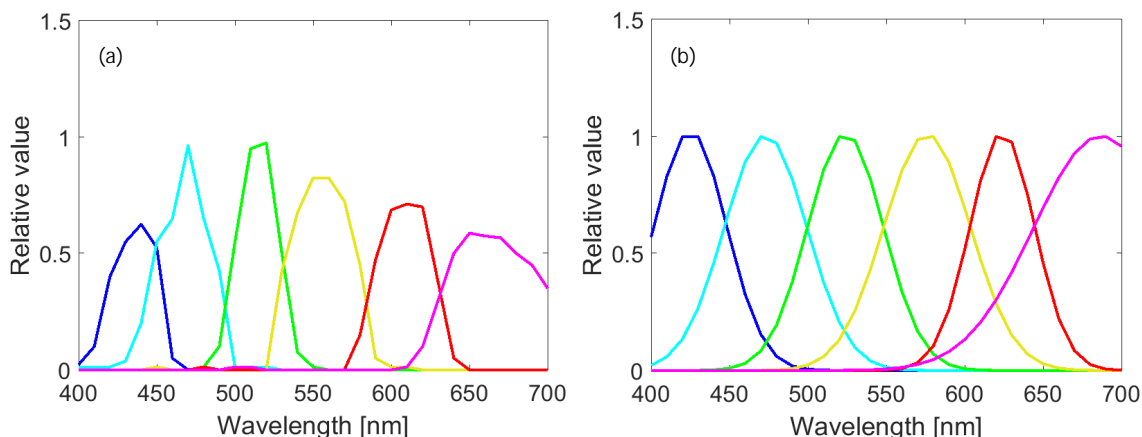


Figure 8: Distribution of six-primary spectra from (a) Ajito *et al.* [2] and (b) Long and Fairchild [3].

Using our selected 3725 samples from the SOCS data, the averaged RMSE value is smaller for our proposed method than the other two methods shown in Figure 9. The averaged RMSE values in selected SOCS data for methods proposed by Ajito *et al.* [2], Long and Fairchild [3], and ours are 0.0636, 0.0204, and 0.0131, respectively. We applied the one-way ANOVA (analysis of variance) to these three methods and obtained $F(2,67047) = 24316.04$, $p < 0.01$, showing that there are significant differences among three methods. Figure 10 shows box plots where a smaller box indicates a higher stability of the values. The open circles outside each box plot indicate the outliers. Outliers are abnormal observations from a sample dataset or population, in the sense that they are greater or less than the applicable upper or lower limits. These limits are typically 1.5 times the box plot length and it could be seen that our proposed method results in the fewest outliers.

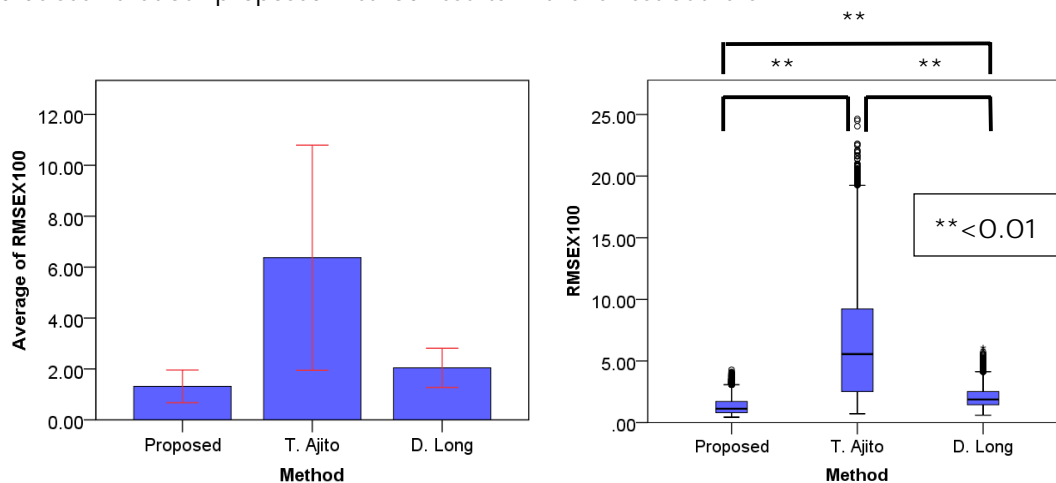


Figure 9 (left): Averaged RMSE results for SOCS samples.

Figure 10 (right): Box plot for SOCS results.

For Macbeth ColorChecker, totally 24 colours were used as we are aiming to improve the reproduction in general situations, we only compared the results for D65 daylight. The corresponding box plot is shown in Figure 11. The results of our proposed method showed significant difference from those of Ajito *et al.* [2], but only small differences from those of Long and Fairchild [3]. The averaged RMSE values in Macbeth ColorChecker in D65 daylight for methods proposed by Ajito *et al.* [2], Long and Fairchild [3], and us are 0.0625, 0.0202, and 0.0202, respectively. The differences among these three values are caused by two factors: the insufficiency sample quantities and the lack of accuracy in some sampling data. For the first factor, we changed the sample data from the original D65 to the 4000-9000 K range with intervals of 20 K for the daylight situation, and the corresponding box plot is shown in Figure 12.

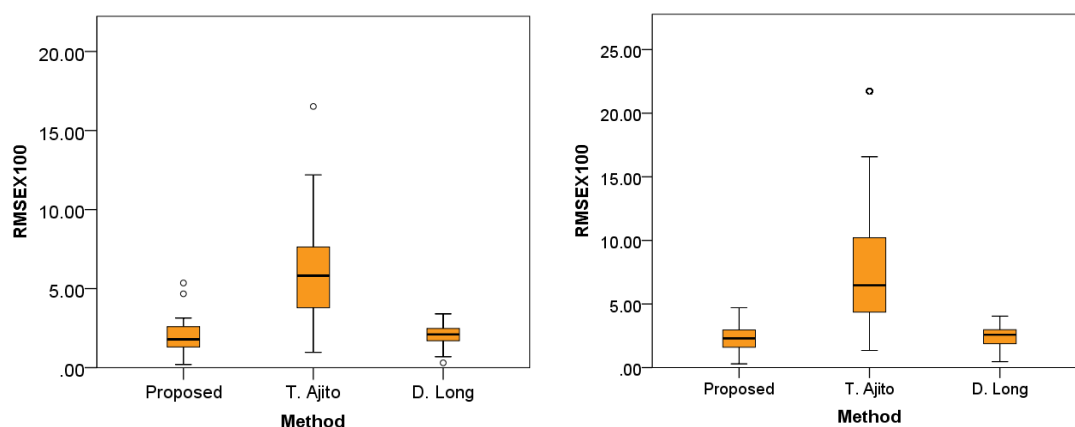


Figure 11 (left): Box plot for Macbeth ColorChecker results in D65 daylight.

Figure 12 (right): Box plot for Macbeth ColorChecker results in 4000-9000 K daylight.

Using one-way ANOVA, we found significant differences among the three models ($F(2,18069) = 7369.69$, $p < 0.01$), with the averaged RMSE values for the methods proposed by Ajito *et al.* [2], Long and Fairchild [3], and us being 0.0785, 0.0243, and 0.0228, respectively. To address the second factor, the lack of accuracy in some sampling data, the reproduction results from the three models are shown in Figures 13(a)-13(c). Four categories defined by Macbeth ColorChecker are considered. Categories 1-4 (Nos. 1-6, 7-12, 13-18, and 19-24) are called the natural, miscellaneous, primary and secondary, and grayscale colours, respectively. Apparently, our method did not reproduce the spectrum well in Categories 2 and 3, as shown in Figures 13(b) and 13(c), respectively.

Apart from the two methods discussed above, there is another numerical optimisation method, called the non-negative matrix factorization (NMF). NMF provides the best non-negative results in the search for an optimal solution [32-34]. It assumed that there exists a non-negative matrix V that can be approximated by the product of two factors W and H , whose relationship is expressed in Equation 12.

$$V \sim WH \quad (12)$$

V and WH followed two mathematical relationships with update rules that are usually called the "multiplicative update rules." Equations 13 and 14 illustrate the relationship between the Euclidean distance of V and WH that can be used to reduce the data difference gradients.

$$W_{ia} \leftarrow W_{ia} \frac{(H^T V)_{ia}}{(H^T W H)_{ia}} \quad (13)$$

$$H_{au} \leftarrow H_{au} \frac{(W^T V)_{au}}{(W^T W H)_{au}} \quad (14)$$

The Euclidean distance of $\|V - WH\|$ follows the update rules, where W and H are composed of $a \times u$, and $i \times a$ terms of the matrix, respectively. Once W and H reach fixed points, the Euclidean distance is also invariant under the update rules. The divergence of $D(\|V - WH\|)$ follows the update rules, where W and H are composed of $a \times u$, and $i \times a$ terms of the matrix, respectively as expressed by Equations 15 and 16.

$$H_{au} \leftarrow H_{au} \frac{\sum_i W_{ia} V_{ia} / (WH)_{iu}}{\sum_k W_{ia}} \quad (15)$$

$$W_{iu} \leftarrow W_{iu} \frac{\sum_i W_{au} V_{iu} / (WH)_{iu}}{\sum_v W_{av}} \quad (16)$$

We set $a = 6$ for six-primary colours and used 1, 5, 10, 20, 40, 80, 200, and 500 iterations to see the differences. Figure 14 shows the obtained averaged RMSE results for the sampled SOCS data after different numbers of iterations. The smallest averaged RMSE value is obtained when the number of iterations is close to 200. We also compared the results for six-primary bands in the 1st (thick lines) and 200th (dotted lines) iterations and found very little change in the band distribution as shown in Figure 15. The colours of the bands correspond to their wavelength peak colours, which are Blue, Cyan, Green, Yellow, Red, and Magenta. We chose to use the results obtained after 200 iterations which have the smallest averaged RMSE value as the six-primary band obtained by the NMF method. We also compared the colour gamut of our proposed method and the NMF method on the CIE (u' , v') chromaticity diagram. The gamut of NMF method in Figure 16(a) is small, the maximal range of covering area is a little bit larger than the sampled SOCS data. Thus, we speculated that this method may only produce results for specifically chosen samples, while the gamut range is likely to be different for different samples. From the result, we think the NMF method is a variable, high uncertainty method, and it is difficult to provide a general combination of spectra for multi-primary display. The gamut range obtained using our proposed method is larger than the SOCS data. Figure 16(b) shows the performance of each spectrum in the three-dimensional CIE (u' , v') chromaticity diagram. The Z axis represents the relative luminance (Y) normalised to 0–100. It could be seen that our maximum relative luminance is similar to that of the NMF method, which is around 60. Moreover, the maximum luminance of Long and Fairchild [3] is higher than that of Ajito *et al.* [2]. Consequently, we posited that our proposed method can provide a general combination of spectra that is broadly applicable in any scenario. In the future, new light sources are likely to be developed, including lasers with wider colour gamut than those currently available. Complete reproduction of these spectra will be a new topic of investigation. Nevertheless, we believe that the method of accurate spectral reproduction proposed here, with its larger gamut, could handle this issue easily.

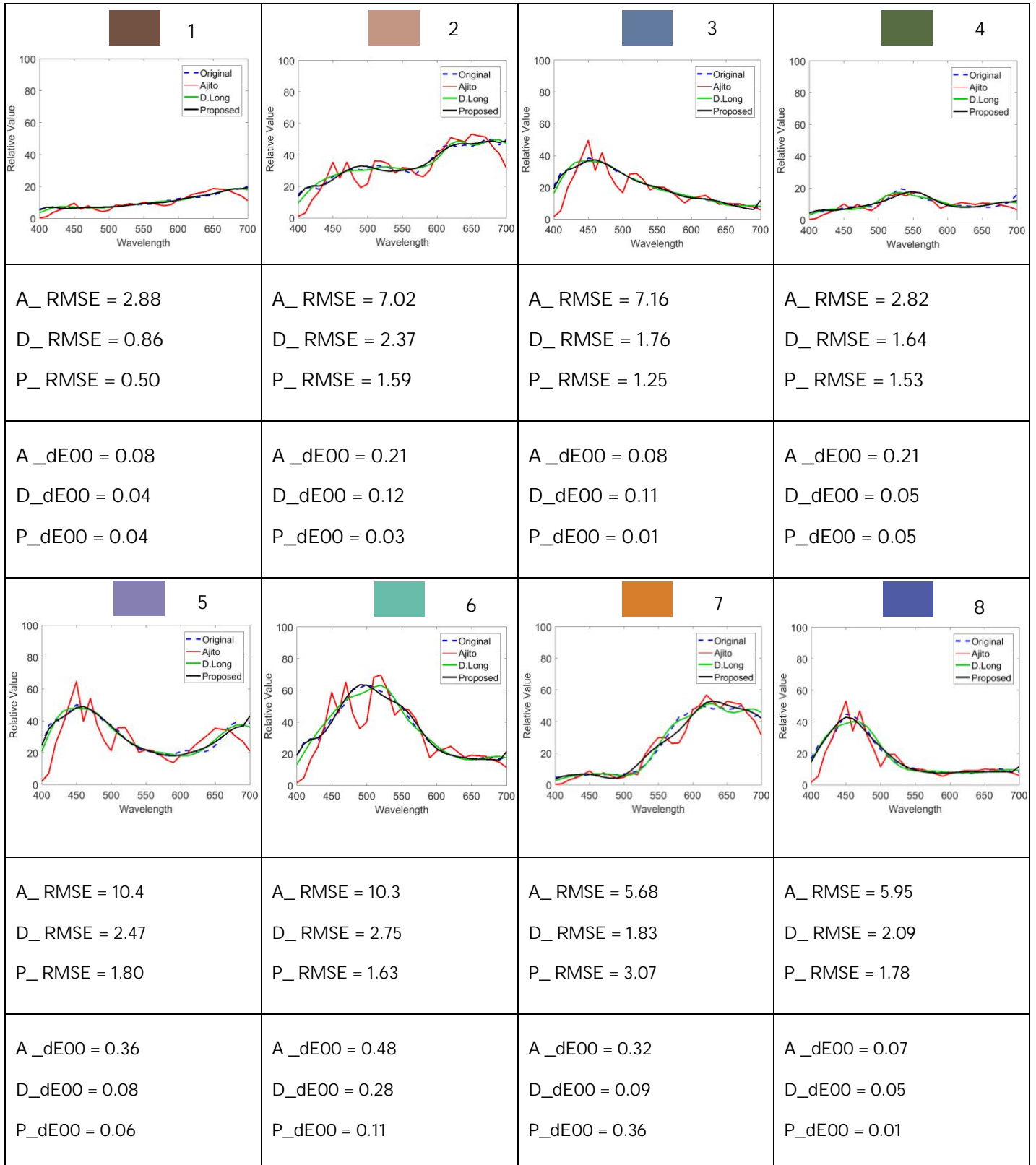


Figure 13: (a) Reproduction for Macbeth ColorChecker Nos. 1-8. Letters A, D, and P denote the results from Ajito et al. [2], Long and Fairchild [3], and the proposed method; the upper and lower columns under each plot show the RMSE and CIEDE2000 results, respectively.

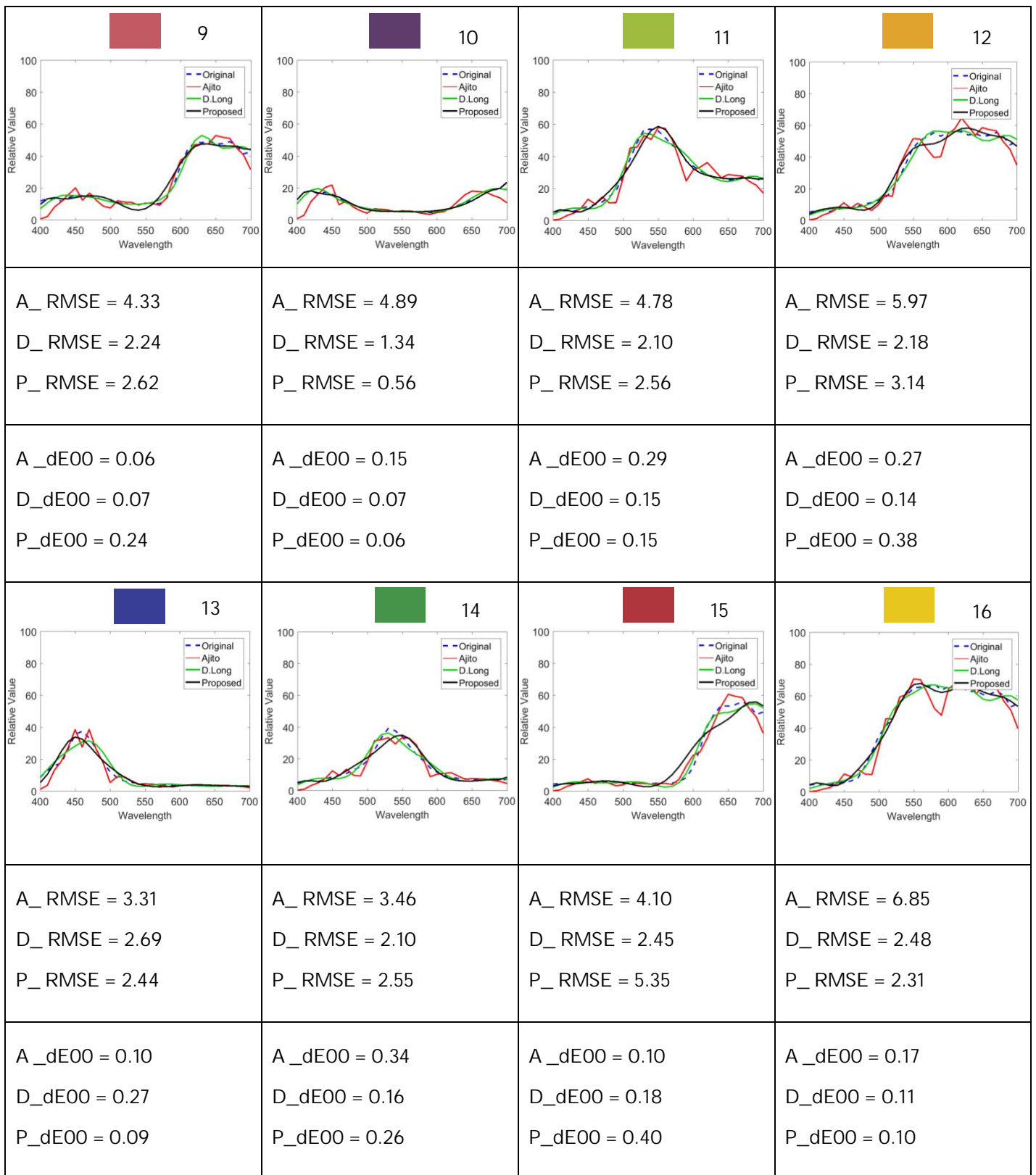


Figure 13: (b) Reproduction for Macbeth ColorChecker Nos. 9-16.

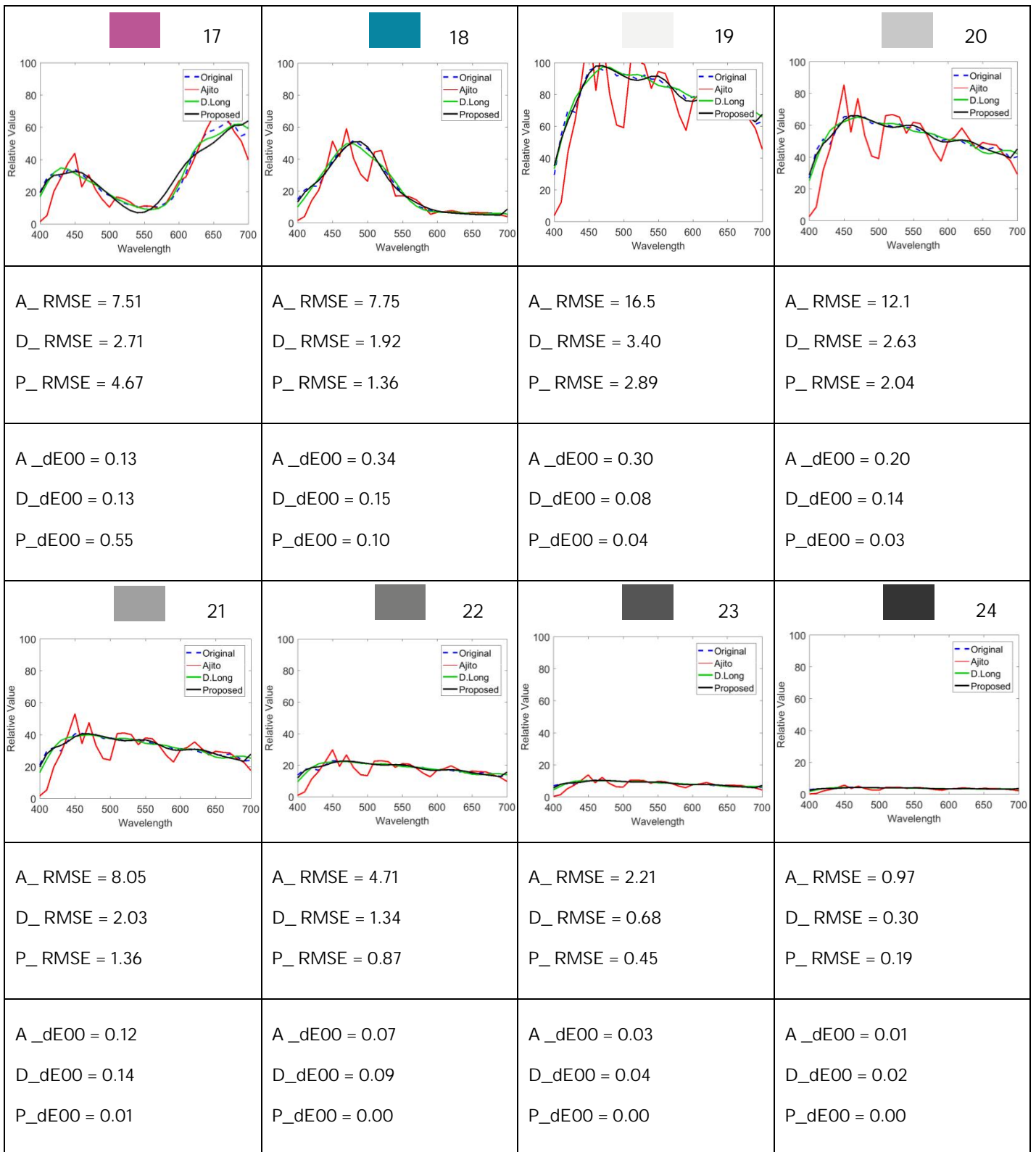


Figure 13: (c) Reproduction for Macbeth ColorChecker Nos. 17-24.

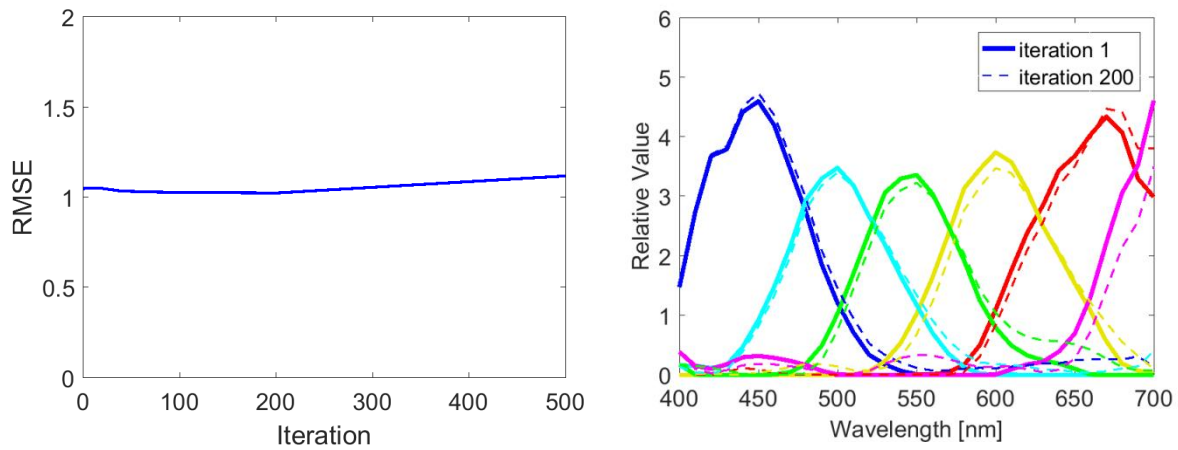


Figure 14: Relation between number of iterations and averaged RMSE in the NMF method.

Figure 15: Six-primary result for 1 and 200 iterations in the NMF method.

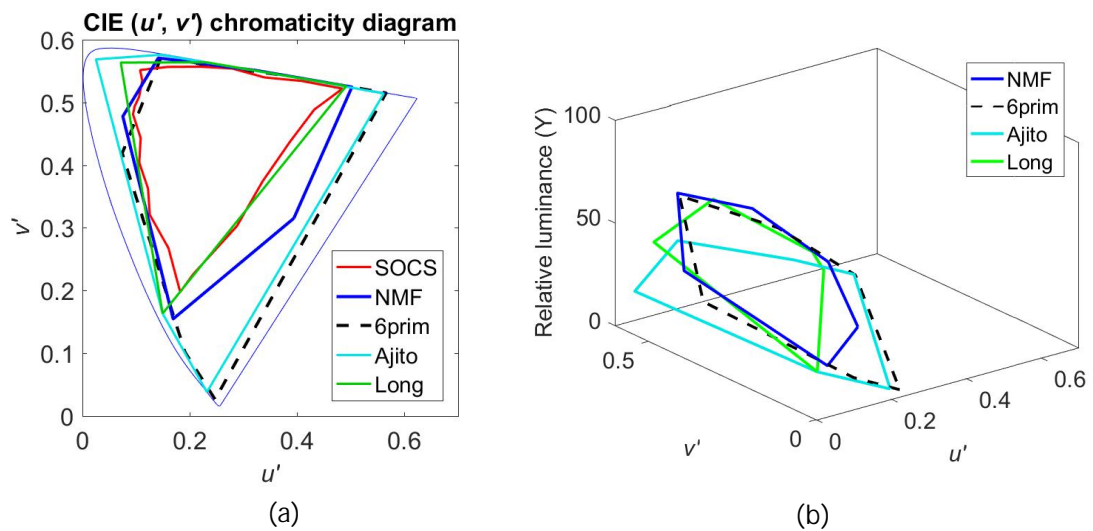


Figure 16: Comparison of SOCS data and results from different methods in CIE (u' , v') chromaticity coordinates: (a) 2-D, (b) 3-D. The red solid, blue solid, cyan solid, green solid and black dotted lines represent the SOCS data, the results from NMF, Ajito et al. [2], Long and Fairchild [3], and the proposed methods; with the areas being 0.07, 0.10, 0.15, 0.08, and 0.14, respectively.

Finally, we sought to evaluate the reproducibility of these four methods for natural spectra. We therefore separated data in the SOCS database into nine categories: Faces, Flowers, Leaves, Paints, Pigments, Photos, Printers, Textiles, and Graphics. With the exception of Flowers, Leaves, Paints, and Pigments which have the smaller amounts of raw data, each category has much more times of data than the sampled SOCS data used in the investigations described above. Here, we used a total of 10751 SOCS samples. All obtained database spectral radiance distributions are products of reflectance and spectral distribution of illumination with the same colour temperatures as for the sampled SOCS data (4000-9000 K, with intervals of 1000 K between 400-700 nm). Each reproduction of the spectral radiance distribution of the natural object colour is determined by the least-squares method, and then its averaged RMSE value is calculated.

Table 3 listed the number of sampled data points and the averaged RMSE values for each category. All methods were based on six primary spectra. The last column shows the average of the four methods. The Photos category has the worst reproducibility, with an RMSE of 4.56 on average, and the Leaves category has the best reproducibility (1.50). Averaged RMSE values for the NMF method are generally better than the other methods, with the exception of Photos category. However, our

proposed method also shows good reproducibility in all categories. The method of Ajito *et al.* [2] has the worst averaged RMSE, which we believe may be related to the early time of the study (circa 1998) and the lack of multi-primary environment. We also believe that the projectors used by Ajito *et al.* [2] were calibrated by the manufacturer for optimal spectral properties, thus it is difficult for our proposed method to completely realise the ideal spectrum. However, we could use a commercial available spectral tunable lighting apparatus that can operate in the multi-band to reproduce the colours. After fixing the six channels only, the normal distribution bands from these methods were passed through this device to see if they could be completely reproduced in reality. Although the averaged RMSE values obtained by our proposed method and that of Long and Fairchild [3] are comparable, the errors obtained by our method are consistently smaller except for the Printers and Graphics categories. The method of Long and Fairchild [3] shows the best performance among all methods in the Graphics category. This might be due to the spectra of the Macbeth ColorChecker were used in the development of that method.

Methods	Categories								
	Faces (496)	Flowers (148)	Leaves (92)	Paints (336)	Pigments (229)	Photos (576)	Printers (3512)	Textiles (2578)	Graphics (2784)
Ajito <i>et al.</i> [2]	6.24	8.06	2.31	8.37	5.46	9.57	4.97	8.62	5.13
Long and Fairchild [3]	2.10	3.09	1.61	2.29	2.21	3.37	2.15	3.19	1.64
NMF	1.33	2.34	1.00	1.72	1.92	3.04	2.09	2.28	1.94
Proposed	1.63	2.53	1.11	1.94	2.53	2.26	2.36	2.46	2.16
Average	2.82	4.00	1.50	3.77	3.03	4.56	2.89	4.13	2.71

Units: averaged RMSE $\times 100$

Table 3: The averaged RMSE values in each category for the four methods.

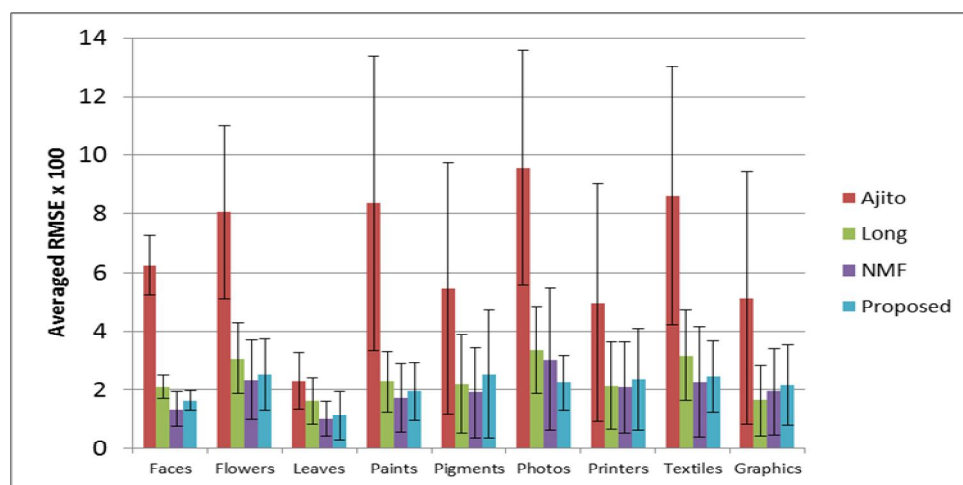


Figure 17: The averaged RMSE values with their error bars in each category for the four methods.

On the other hand, the smoothness of the spectra can be seen as the continuity of a set of data, and it could be assessed using the error bar of the reproduced spectra. Figure 17 shows the average RMSE values with their error bars by category. The data for Ajito *et al.* [2] had the worst smoothness compared to the other three sets. Our proposed method had the best smoothness, especially in Faces, Paints, Photos and Textiles categories. In Flowers category, our proposed method is comparable to that of Long and Fairchild [3] and better than the other two. In addition, the method of Long and Fairchild [3] is superior to the other three methods in Printers and Graphics categories. As for the NMF method, it performed better than the other three only in the Leaves category, showing great instability.

In addition, we also wanted to find out how well the three methods (NMF and those proposed by Ajito *et al.* [2] and Long and Fairchild [3]) reproduce data under other light sources in comparison to our method. We prepared three light sources: the CIE standard illuminant F1 (6450K fluorescent lamp), the Toshiba E-Core Par30s (6500K LED bulb), and Philips 50Par30L (2750K tungsten halogen lamp). The spectral distributions of three light sources are represented in Figures 18(a)-18(c). The radiant powers were normalised to 0–1, and the wavelength range was from 400 to 700 nm at 10 nm intervals. The averaged RMSE for three light sources are shown in Tables 4-6. It could be seen that the RMSE values of our proposed method are only slightly more than 3 among three light sources that showed stable reproducibility. The method of Ajito *et al.* [2] has the best reproducibility for the LED bulb, and we think it might related to the properties of their chosen projectors' primary colours. The method of Long and Fairchild [3] performed perfectly for the fluorescent lamp. Its performance is also similar to our proposed method for the tungsten halogen lamp, but the reproducibility was lower for the LED bulb.

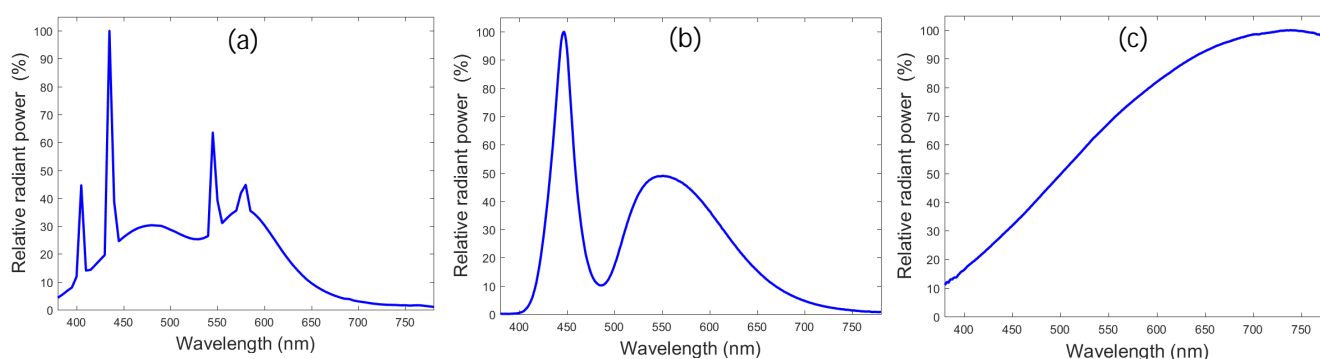


Figure 18: Spectral distributions of three light sources: (a) CIE standard illuminant F1, (b) Toshiba E-Core Par30s, (c) Philips 50Par30L.

Methods	Categories								
	Faces (496)	Flowers (148)	Leaves (92)	Paints (336)	Pigments (229)	Photos (576)	Printers (3512)	Textiles (2578)	Graphics (2784)
Ajito <i>et al.</i> [2]	2.13	1.96	0.81	2.84	1.77	2.07	1.25	0.90	1.48
Long and Fairchild [3]	0.96	1.05	1.34	1.34	0.90	0.99	0.78	0.46	0.79
NMF	1.05	1.22	1.06	1.85	1.20	1.21	0.90	0.56	0.93
Proposed	1.65	1.53	0.78	2.16	1.45	1.44	0.92	0.65	1.03
Average	1.44	1.44	0.99	2.04	1.33	1.42	0.96	0.64	1.05

Units: averaged RMSE \times 100

Table 4: The averaged RMSE values of F1 fluorescent lamp in each category for the four methods.

Methods	Categories								
	Faces (496)	Flowers (148)	Leaves (92)	Paints (336)	Pigments (229)	Photos (576)	Printers (3512)	Textiles (2578)	Graphics (2784)
Ajito <i>et al.</i> [2]	2.55	2.61	0.81	3.61	2.09	2.50	1.75	2.62	2.16
Long and Fairchild [3]	3.70	3.62	1.34	5.54	2.46	4.05	2.67	3.98	3.36
NMF	3.20	3.23	1.06	4.79	2.29	3.47	2.47	3.47	3.03
Proposed	2.45	2.54	0.78	3.67	2.06	2.66	1.95	2.73	2.33
Average	2.97	3.00	0.99	4.40	2.22	3.17	2.21	3.20	2.72

Units: averaged RMSE \times 100

Table 5: The averaged RMSE values of LED bulb in each category for the four methods.

Methods	Categories								
	Faces (496)	Flowers (148)	Leaves (92)	Paints (336)	Pigments (229)	Photos (576)	Printers (3512)	Textiles (2578)	Graphics (2784)
Ajito <i>et al.</i> [2]	5.37	8.54	2.09	5.24	4.81	8.32	4.02	7.3	3.23
Long and Fairchild [3]	1.12	2.87	1.47	1.01	1.5	2.72	1.79	2.8	0.6
NMF	1.36	2.3	1.05	1.25	1.61	1.65	1.54	1.63	1.14
Proposed	0.99	2.61	1.4	1.3	1.98	1.85	2.02	2.42	1.3
Average	2.21	4.08	1.50	2.2	2.47	3.63	2.34	3.53	1.56

Units: averaged RMSE \times 100

Table 6: The averaged RMSE values of tungsten halogen lamp in each category for the four methods.

The NMF method is fast, highly accurate, and provides an optimal combination of bands for given samples. However, the obtained band distributions are irregular for the blue and red bands in Figure 15. The same trends could be seen for the other light sources: some light sources performed well while some did not, showing the method's instability. If we used programmable output light source devices to modify the corresponding optimal combination of bands, the bands could not be simulated by mathematical formula exactly. In comparison, our proposed method could provide an optimal combination of bands for these devices and reproduce the spectra of natural colours better than the other methods.

Conclusions

In this study, we first used the PCA method to reproduce a large spectral reflectance dataset, and found that the data were represented well by three principal components. Second, using the least-squares method, we fitted six primaries with a normal distribution to the spectral radiance data that consisted the combination of reflectance and illumination data. The averaged RMSE values and colour differences of the reproduction were 0.0132 and 0.08, respectively which represented good results.

Compared to the bands reproduced using the methods of Ajito *et al.* [2] and Long and Fairchild [3], our proposed method produced good results with lower averaged RMSE values, and with significant differences from other methods showed by using ANOVA analysis. The proposed method could reproduce better spectra of natural objects. The quality of colorimetric reproduction usually depends on their different colour values between the original and reproduction. Although lower averaged RMSE values do not directly correspond to good colorimetric reproduction, the averaged colour differences obtained using our proposed method are smaller than those from using other methods. Hence, the differences in colour appearance owing to metamerism will be eliminated, yielding good colour reproduction.

While the NMF method provides the optimal combination of bands, its results are irregular compared to those from the other methods. We believe that if rough band distributions are obtained, it is difficult to reproduce the same bands. The method of Long and Fairchild's [3] and ours can precisely provide the numerical parameters of the Gaussian function and normal distribution function, respectively. These methods could quickly reproduce the spectra by using devices that can adjust the spectral radiance distribution by numerical algorithm.

Although the results from Ajito *et al.* [2] occupy the largest gamut area in the in the CIE (u' , v') chromatic diagram, the reproduction is the least accurate among the four methods. Our proposed method has an appropriately sized area in the diagram, highly smooth spectral distribution, and good

reproduction result. The relative luminance is also the highest. Band data obtained from this method can reproduce well the spectral radiance distributions for the SOCS data.

Even though we used daylight data with a limited number of colour temperatures as samples, excellent reproducibility was also obtained in the spectral reproduction of other light sources.

We believe it can be used in technological applications including some mentioned in Introduction. The method allows effective reproduction of original spectral targets and can be used to develop state-of-the-art filters for novel types of displays that extend beyond the LCDs and LEDs.

References

- Judd DB, MacAdam DL, Wyszecki G, Budde HW, Condit HR, Henderson ST and Simonds JL (1964), Spectral distribution of typical daylight as a function of correlated color temperature, *Journal of the Optical Society of America A*, **54** (8), 1031-1040.
- Ajito T, Obi T, Yamaguchi M and Ohshima N (2000), Expanded color gamut reproduced by six-primary projection display, *Proceedings of the SPIE The International Society of Optical Engineering*, **3954**, 130-139.
- Long D and Fairchild MD (2011), Optimizing spectral color reproduction in multi-primary digital projection, *Proceedings of the IS&T/SID's Nineteenth Color and Imaging Conference*, 290-297, San Jose (USA).
- Kubono A, Kyokane Y, Akiyama R and Tanaka K (2001), Effect of cell parameters on the properties of hybrid twisted nematic displays, *Journal of Applied Physics*, **90** (12), 5859-5865.
- Teragawa M, Yoshida A, Yoshiyama K, Nakagawa S, Tomizawa K and Yoshida Y (2012), Multi-primary-color displays: The latest technologies and their benefits, *Journal of the Society for Information Display*, **20** (1), 1-11.
- Lee SH, Kim HY, Lee YH, Park IC and Rho BG (1998), Wide viewing angle, homeotropic nematic liquid-display controlled by effective field, *Journal of Applied Physics Letters*, **73** (4), 470-472.
- Lee B-W, Ju Y-G, Hwang YI, Lee H-Y, Kim CW, Lee JS and Souk JH (2009), Micro-cavity design of bottom-emitting AMOLED with white OLED and RGBW color filters for 100% color gamut, *Journal of the Society for Information Display*, **17** (2), 151-157.
- Konig F, Ohsawa K, Yamaguchi M, Ohshima N and Hill B (2002), A multiprimary display: optimized control values for displaying tristimulus values, *Proceedings of the IS&T's Image Processing, Image Quality, Image Capture, Systems (PICS) Conference*, 215-220, Portland (USA).
- den Engelsen D, Heynderickx I and Sluyterman S (2004), Color-gamut expansion in CRTs, *Journal of the Society for Information Display*, **12** (3), 241-250.
- Choe W, Lee S-D and Kim C-Y (2005), Studying for multiprimary LCD, *Proceedings of the SPIE The International Society of Optical Engineering*, **5667**, 336-343.
- Roosendaal SJ, Tol EVD, Langendijk EHA, Hector JR, Hughes JR, Inoue M, Fujimoto H, Watanabe H, Nasu K, Inada T, Yoshiga M, Naitoh S, Shibasaki M, Kawata S and Sumi N (2005), A wide gamut, high aperture mobile spectrum sequential liquid crystal display, *SID 05 Digest*, 1116-1119.
- Yang Y-C, Song K-K, Rho S-G, Rho N-S, Hong S-J, Deul K-B, Hong M-P, Chung K-H, Choe W-H, Lee S-D, Kim C-Y, Lee S-H and Kim H-R (2005), Development of Six-primary LCD, *SID 05 Digest*, 1210-1213.
- Chino E, Tajiri K, Kawakami H, Ohira H, Kamijo K, Kaneko H, Kato S, Ozawa Y, Kurumisawa T, Inoue K, Endo K, Moriya H, Aragaki T and Murai K (2006), Development of wide-color-gamut mobile displays with four-primary-color LCDs, *SID 06 Digest*, 1223-1224.
- Ueki S, Nakamura K, Yoshida Y, Mori T, Tomizawa K, Narutaki Y and Itoh Y (2009), Five-primary-color 60-inch LCD with novel wide color gamut and wide viewing angle, *SID 09 Digest*, 927-930.
- Cheng H-C, Ben-David I and Wu S-T (2010), Five-Primary-Color LCDs, *Journal of Display Technology*, **6** (1), 3-7.

16. Luo Z and Wu S-T (2014), A spatiotemporal four-primary color LCD with quantum dots, *Journal of Display Technology*, **10** (5), 367-372.
17. Chang C-K, Mizokami Y, Yaguchi H, Sun P-L and Chen H-S (2017), Effect of gamut expansion of object colours on a simulated six-primary display, *Journal of the International Colour Association*, **18**, 1-17.
18. Hunt RWG (1970), Objectives in color reproduction, *The Journal of Photographic Science and Engineering*, **18**, 205-215.
19. Hunt RWG (2004), *The Reproduction of Colour*, Sixth Edition, John Wiley and Sons.
20. Ben-Chorin M and Eliav D (2007), Multi-primary design of spectrally accurate displays, *Journal of the Society for Information Display*, **15** (9), 667-677.
21. Li Y, Majumder A, Lu D and Gopi M (2015), Content-independent multi-spectral display using superimposed projections, *Computer Graphics Forum*, **34**, 337-348.
22. Murakami Y, Ishii J, Obi T, Yamaguchi M and Ohyama N (2004), Color conversion method for multi-primary display for spectral color reproduction, *Journal of Electronic Imaging*, **13** (4), 701-708.
23. JIS - TR X 0012, Japanese Industrial Standards Association (1998).
24. Hotelling H (1933), Analysis of a complex of statistical variables into principal components, *Journal of Educational Psychology*, **24** (6), 417-441.
25. Cohen J (1964), Dependency of the spectral reflectance curves of the Munsell color chips, *Psychonomic Science*, **1** (1-12), 369-370.
26. Maloney LT (1986), Evaluation of linear models of surface spectral reflectance with small numbers of parameters, *Journal of the Optical Society of America A*, **3** (10), 1673-1683.
27. Mizokami Y and Webster MA (2012), Are Gaussian spectra a viable perceptual assumption in color appearance?, *Journal of the Optical Society of America A*, **29** (2), A10-A18.
28. Dannemiller JL (1992), Spectral reflectance of natural objects: how many basis functions are necessary?, *Journal of the Optical Society of America A*, **9** (4), 507-515.
29. Nascimento SM, Foster DH and Amano K (2005), Psychophysical estimates of the number of spectral-reflectance basis functions needed to reproduce natural scenes, *Journal of the Optical Society of America A*, **22** (6), 1017-1022.
30. Vrhel MJ, Gershon R and Iwan LS (1994), Measurement and analysis of object reflectance spectra, *Color Research and Application*, **19** (1), 4-9.
31. Luo MR, Cui G and Rigg B (2001), The development of the CIE 2000 colour-difference formula: CIEDE2000, *Color Research and Application*, **26** (5), 340-350.
32. Lee DD and Seung HS (1999), Learning the parts of objects by non-negative matrix factorization, *Nature*, **401**, 788-791.
33. Lee DD and Seung HS (2001), Algorithms for non-negative matrix factorization, *Proceedings of the Conference on Neural Information Processing Systems*, **13**, 556-562.
34. Berry MW, Browne M, Langville AN, Pauca VP and Plemmons RJ (2007), Algorithms and applications for approximate nonnegative matrix factorization, *Computational Statistics and Data Analysis*, **52**, 155-173.